International Journal of Applied Earth Observations and Geoinformation 108 (2022) 102728

Contents lists available at ScienceDirect

International Journal of Applied Earth Observations and Geoinformation

journal homepage: www.elsevier.com/locate/jag

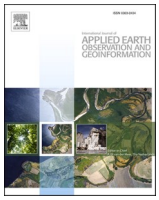

Evaluating the effect of DEM resolution on performance of cartographic depth-to-water maps, for planning logging operations

Sima Mohtashami [a,*], Lars Eliasson [a], Linnea Hansson [a], Erik Willén [a], Tomas Thierfelder [b], Tomas Nordfjell [c]

[a] The Forestry Research Institute of Sweden, Skogforsk, Uppsala, Sweden
[b] Department of Energy and Technology, Swedish University of Agricultural Sciences (SLU), Uppsala, Sweden
[c] Department of Forest Biomaterials and Technology, Swedish University of Agricultural Sciences (SLU), Umeå, Sweden

ARTICLE INFO

Keywords:
Soil moisture maps
DTW
Digital Elevation Model
Forestry
Soil disturbance

ABSTRACT

Reliable and accurate soil moisture maps are needed to minimise the risk of soil disturbance during logging operations. Depth-to-water (DTW) maps extracted from digital elevation models have shown potential for identifying water flow paths and associated wet and moist areas, based on surface topography. We have examined whether DEMs from airborne LiDAR data with varying point density can improve performance of DTW maps in planning logging operations. Soil moisture content was estimated on eight sites after logging operations and compared to DTW maps created from DEMs with resolutions of 2 m, 1 m, and 0.5 m. Different threshold values for wet soil (1 m and 1.5 m depth to water) were also tested. The map performances, measured by accuracy (ACC) and Matthews Correlation Coefficient (MCC), changed slightly (79%, 81% and 82% and 0.33, 0.26 and 0.30 respectively) when DEM resolutions varied from 2 m to 1 m, and 0.5 m. The corresponding values when the DTW threshold value for wet/dry soil changed from 1 m to 1.5 m were 70%, 72%, 71% and 0.38, 0.41 and 0.39. LiDAR-based DEM resolutions of 1–2 m were found to be sufficient for extraction of DTW maps during planning of logging operations, when knowledge about soil hydrological features, associated wet and moist areas, and their connectivity is beneficial.

1. Introduction

Utilising forestry machines in combination with a warming climate requires extra efforts to avoid possible soil disturbances during logging operations in forests (Uusitalo et al., 2020). Reliable and accurate soil moisture maps, based on high resolution digital elevation models (DEM), are among tools that improve planning and execution of logging operations (Hoffmann et al., 2022). Capturing topographic details of ground surface from point clouds collected by airborne Light Detection and Ranging (LiDAR) has contributed to DEM extractions with improved resolution and information contents (Wehr & Lohr, 1999). Which point density LiDAR data and corresponding DEM resolution to use is an important question for practical forestry, as the DEMs are used for creating different kinds of trafficability maps. For example, soil moisture maps are used in most heavy forestry machines in Sweden today (Ring et al., 2020; Ågren et al., 2021;).

Logging operations in Swedish forestry have developed considerably since the 1940s. Human and horse muscles were first replaced with chain-saws and modified farm tractors, which gradually developed to the current use of forest machines. Improved productivity, cost-efficiency, ergonomics and work safety of the operations and higher demands for wood-based-products from forests were the main drivers of this development (Nordfjell et al., 2019). Simultaneously, forest machines have become bigger and heavier, weighing approximately 15–40 Mg, which implies a higher risk of soil disturbances, i.e. rutting, compaction, runoff, and erosion (Cambi et al., 2015). The risk for soil disturbances intensifies when forest soils are wet and moist (Toivio et al., 2017). In the boreal forest of Nordic regions, periods with frozen soils and improved bearing capacity are likely to diminish due to anticipated warmer climate conditions (Lehtonen et al., 2019), underlining the need for improved planning of logging operations in sensitive areas. Soil moisture content, together with soil texture, are important factors for determining soil bearing capacity (Susnjar et al., 2006; Wästerlund, 2020), i.e., the ability of soil to withstand external forces without undergoing detrimental changes. Deep ruts develop more easily on fine-grained soils (Eliasson & Wästerlund, 2007; Sirén et al., 2019)

* Corresponding author.
E-mail address: sima.mohtashami@skogforsk.se (S. Mohtashami).

https://doi.org/10.1016/j.jag.2022.102728
Received 22 December 2021; Received in revised form 1 February 2022; Accepted 17 February 2022
Available online 4 March 2022

and peatlands (Uusitalo & Ala-Ilomäki, 2013) with high moisture content. Ruts can cause water ponding on flat terrain due to compaction and reduced hydraulic conductivity in machine tracks, leading to increased runoff and sediment transport to nearby watercourses (Hansson et al., 2018). Erosion rate may increase after machine passages in steep terrain (Labelle et al., 2021; Najafi et al., 2009), creating extra obstacles to the natural recovery of soils for decades after off-road transportations (DeArmond et al., 2021).

The spatial variation of soil moisture content is influenced by soil texture, topography (measured as slope and elevation), and vegetation, and varies temporally according to meteorological condition, i.e., temperature and precipitation (Huisman et al., 2002; Lunt et al., 2005). Knowledge about the location of sensitive soils with high moisture content is therefore necessary to minimise negative impact caused by off-road transportation (Campbell et al., 2013; Jones & Arp, 2019; Murphy et al., 2009). Measuring soil moisture content using in-situ techniques like time domain reflectometry (TDR) or ground penetrating radar (GPR) to measure soil moisture content over large areas (hectares) are time- and labour-intensive (Lekshmi et al., 2014), making these methods non-practical for operational forestry planning. Soil moisture prediction models, using digital elevation models (DEM) based on increasingly available LiDAR technology, or photogrammetry-based DEMs, have therefore been used to improve the mapping of soil hydrological features.

The topographic wetness index (TWI) (Beven & Kirkby, 1979) was among pioneer wetness models that used topography to model water flow paths in landscape. The index is calculated by relating upslope catchment area at each DEM cell to a calculated slope in that cell. TWI was shown to be more sensitive to proper estimation of upslope areas than the calculated local slope at different resolutions (Hjerdt et al., 2004). This property makes the index sensitive to underlying DEM resolution and reduces the accuracy of soil moisture estimation in less elevated areas, where local slope does not reflect the hydraulic gradient efficiently (Grabs et al., 2009). TWI was shown to function properly for large-scale landscape planning, but to lose its robustness at high DEM resolutions (Sørensen & Seibert, 2007; Ågren et al., 2014).

Depth-to-water (DTW) index is another DEM-based soil wetness index that calculates least elevation difference between surface flow channels and nearby landscape areas (Murphy et al., 2007; Murphy et al., 2008). The surface flow channels, extracted from DEMs, are regarded as reference ground water level by DTW index. DTW values are defined as zero at surface flow channels. Moving upwards from flow channels in the landscape implies increased depth to water values, indicating reduced soil wetness away from surface waters. Soil moisture maps based on the DTW index therefore need assigning two thresholds: 1) flow initiation area (FIA), i.e., a catchment area required to form flow channels, 2) a DTW threshold value for when soils are wet, i.e., a high soil moisture content on a time-averaged basis. Ågren et al. (2014) compared DTW maps of different FIA values, TWI, and seven other DEM-derived indexes (at resolutions ranging from 2 to 100 m) to measure soil moisture classes in the field in a Swedish boreal forest catchment area. They reported DTW as the most numerically robust index to predict soil moisture classes. Identification and connectivity of smaller wetlands areas (<1 ha) and riparian zones extracted from 10-m photogrammetry-based DEM were improved using the DTW index, compared to aerial photo interpretations (Murphy et al., 2007). Much longer stream flow channels could also be mapped in Sweden, both at watershed (Ågren et al., 2015) and national scales (Ågren & Lidberg, 2019), using the DTW index. The stream flow channels were extracted from 2-m DEMs and compared to aerial photo-based flow channels shown on topographic maps (scale of 1: 12 500) created by the Swedish Mapping, Cadastral and Land Registration Authority.

DTW maps can help logging planners decide the proper time to perform logging operations on logging sites with large areas of moist and wet soils. Logging operations in these areas can be scheduled during winter periods when the soil is frozen and has greater strength for machine passages (Mattila & Tokola 2019; Susnjar et al., 2006). When DTW maps are used to identify moist and wet areas in logging sites, the risk for rutting may be reduced if machine operating trails do not cross such areas (Arp, 2009; White et al., 2013). Leaving logging residues on machine operating trails (Labelle et al., 2021) improves soil bearing capacity in these areas, prior to necessary machine passages. The planning measures become extra important when logging sites are in the vicinity of groundwater discharge hotspots with high ecological values (Kuglerová et al., 2014). DTW maps were found to be an effective tool for minimising severe rutting in areas close to surface waters (Friberg & Bergkvist, 2016), although they cannot predict rut locations in logging operations (Mohtashami et al., 2017; Schönauer et al., 2021a; Ågren et al., 2015).

DTW maps can also be used to develop soil trafficability models. In a case study in Canada, Campbell et al. (2013) related cone penetration index to rut depth, DEM-derived elevation, slope, and DTW index (at 2-m resolution), creating projected rut-depth maps for an all-terrain vehicle navigation in forest. The model was further improved by including hydrologically predicted soil moisture content and meteorological data to adjust the model for actual weather conditions (Jones & Arp, 2019). Despite indicating promising applications in the study areas, the authors stated that further evaluation in different terrain conditions was required.

Soil moisture maps are also important in forestry for identifying suitable locations for necessary stream crossings (Ring et al., 2020). Soil moisture maps could be used for designing optimal and functional forest buffers/riparian zones around permanent or temporal stream flow networks with important ecological values (Kuglerová et al., 2017; Kuglerová et al., 2014). They could also be used to improve planning of site preparation and fertilisation adjacent to surface waters (Ring et al., 2020; Ågren et al., 2015). Reliable and accurate soil moisture maps could therefore lead to essential improvements in planning of logging operations.

Creating DTW maps that capture temporal and spatial variations of stream networks and associated wet areas at both small and large scales is challenging. To improve the map performance and customise them to local and temporal conditions, the FIA threshold can be adjusted to local physiographic properties (Murphy et al., 2009; Ågren & Lidberg, 2019) and seasonal changes (Schönauer et al., 2021b; Ågren et al., 2015). The DTW threshold value for separating wet/dry soil also needs to be adjusted to soil drainage properties, topography, and local weather conditions (Ågren et al., 2021). DTW values of 1 m (Ågren et al., 2014, Murphy et al., 2011) or 1.5–1.7 m (Murphy et al., 2009) have traditionally been used for this purpose in different studies. How the change of threshold may affect the performance of DTW maps in the same areas has not been specifically reported in previous studies.

Resolution and information content of DEMs are important factors affecting extraction of hydrological features (MacMillan et al., 2014). A comparison between the performance of DTW index and soil wetness index (SWI) using LiDAR-based DEM (1-m resolution) and photogrammetry-based DEM (10-m resolution) indicated that a higher DEM resolution resulted in improved conformance for both moisture models (Murphy et al., 2009). Lidberg et al. (2017) evaluated different pre-processing methods on LiDAR DEMs with resolutions of 16 m, 8 m 4 m and 2 m, and showed that higher DEM resolution leads to more accurate stream network extractions. Stream-road crossings identified in DEMs were compared with field recorded culvert positions in this study. Previous studies have not addressed how an even higher resolution than 1 or 2 m of DEMs created from higher point density LiDAR data can affect the performance of the DTW maps to identify wet and moist areas and the potential to improve the maps for planning forest operations.

The objective of this study is therefore to evaluate the effect of high-resolution DEM (2 m, 1 m, 0.5 m), based on airborne LiDAR data, hereafter LiDAR data, with different point density (0.5–1-point m^{-2}, 1–2-point m^{-2}, and 24-point m^{-2}), on soil moisture prediction using a cartographic depth-to-water (DTW) index, and an empirical approach.

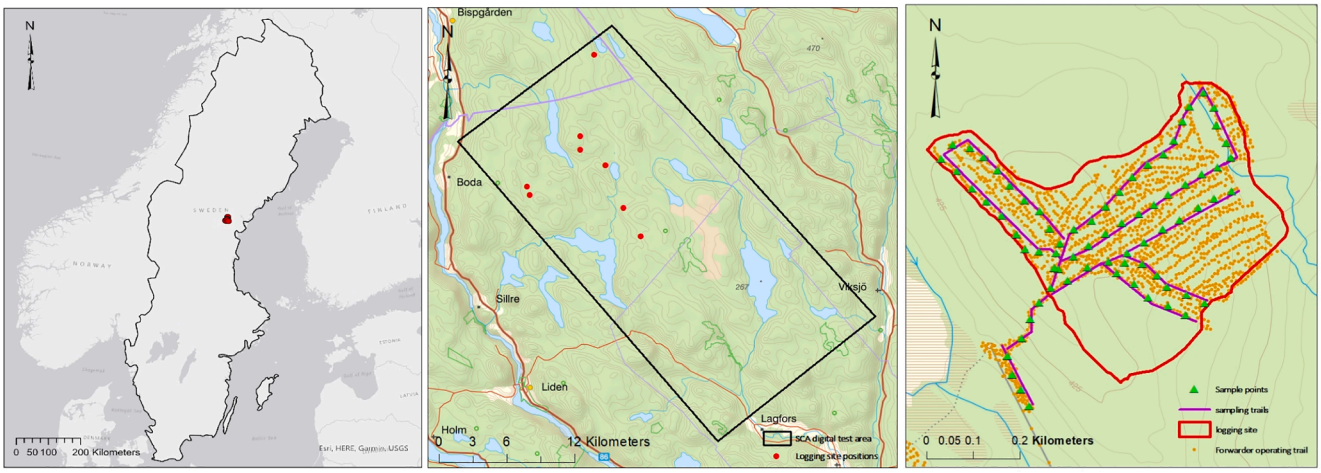

Fig. 1. Left: Overview of the logging sites, in mid-eastern Sweden. Centre: Distribution of the logging sites within the SCA digital test. Right: One of the studied logging sites over the topographic map. Data about soil moisture points were collected in geopositioned sample points (green triangles) along pre-marked sampling paths (purple), selected on the basis of forwarder time logged operating trails (small orange dots).

Table 1
Description of surveyed logging sites with information on logging site area (ha), main soil type according to Quaternary Deposits maps, and number of collected sample points.

Site No.	Area (ha)	Main soil type	No. of collected sample points
1	7.2	Till	36
2	5.2	Till	26
3	23.6	Till	70
4	17.8	Till	44
5	6.5	Peat	43
6	17.8	Till, bedrock	66
7	15.8	Till	59
8	10.2	Bedrock, Peat	41

This is done by point-to-point comparison of field estimated soil moisture with DTW-based soil moisture predictions with resolutions of 2 m, 1 m, and 0.5 m on eight logging sites in mid-eastern Sweden, after logging operations. Another objective was to test whether the results would change when the threshold value for wet soil was changed from 1 m to 1.5 m DTW.

2. Materials and methods

2.1. Study areas

The study included eight logging sites selected from 24 recent final fellings in the SCA forest company's digital test site (17°2′47″E, 62°49′46″N) in mid-eastern Sweden (Fig. 1). The sites were selected to ensure a variation of estimated soil texture and soil moisture according to available digital maps. The logging sites varied in size and topographic condition (elevation, slope), and were situated mainly on mineral till soils according to Quaternary Deposits maps (1: 25000–1:100 000 Geological Survey of Sweden). The dominating tree species were Norway spruce (Picea abies (L.) Karst.) and Scot's pine (Pinus sylvestris L.). The logging sites were clear-cut during spring-summer 2020, applying a cut-to length (CTL) mechanised system, using harvester models Komatsu 951 and JD 1470 G (27–30 Mg) and forwarders, Komatsu 895, and JD 1910 G models (50–52 Mg when fully loaded). A general description of the logging sites is provided in Table 1.

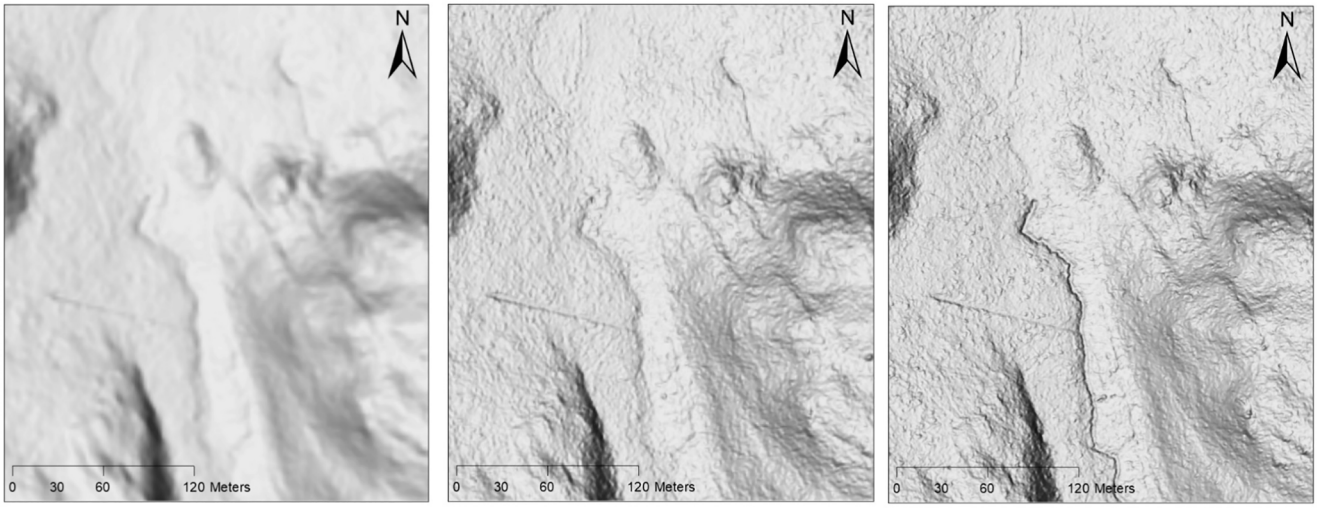

Fig. 2. Digital elevation models (DEM) with resolutions of 2 m (left), 1 m (middle) and 0.5 m (right) presented by multiple hillshade effect. Illustration of surface detail improves when DEMs are illuminated with light from six different directions, i.e., multiple hillshading. A man-made ditch (black line) is captured more clearly by 0.5 m DEM.

Table 2
Technical description of airborne LiDAR data used in terms of point density, laser scanner model, manufacturer, and LiDAR accuracy. DEM extraction algorithm and provider of each data source are also specified.

DEM resolution (m)	LiDAR data point density (point m^{-2})	Laser scanner model, manufacturer	LiDAR Accuracy	DEM extraction algorithm	Data Provider
2	0.5–1	ALS 60, Leica	XY accuracy < 0.3 Vertical accuracy = 0.1 m	Triangular Irregular Network (TIN) interpolation	Swedish mapping, cadastral and land registration authority (Anon, 2020)
1	1–2	LS1A, Leitech	XY accuracy < 0.3 Vertical accuracy < 0.1 m	Gridding with adaptive triangulation	Swedish mapping, cadastral and land registration authority (Anon, 2021)
0.5	24	VQ-1560i DW, RIEGL	XY accuracy = 0.02 m Vertical accuracy = 0.02 m	Streaming Triangular Irregular Network interpolation	SCA forest company (Anon, 2022)

Table 3
Mean value and standard deviation of elevation and slope within the studied logging sites, extracted from 2 m DEM.

Logging site No.	Elevation (m)		Slope (degrees)	
	Mean	Standard deviation	Mean	Standard deviation
1	366.11	3.48	6.68	4.05
2	364.50	4.06	8.90	7.35
3	419.54	8.19	7.02	3.74
4	340.70	6.63	9.77	6.70
5	373.35	5.22	11.16	7.05
6	367.03	9.56	12.25	8.05
7	387.07	9.9	7.09	3.86
8	341.14	12.98	11.54	6.63
Average	369.93	7.50	9.30	5.93

2.2. Field data collection

Soil moisture was estimated in the field during September-November 2020. The sampling paths were pre-marked on digital topographic maps along the time-logged forwarder operating trails to make data inventory practical (Fig. 1). Soil moisture in the field was estimated and classified as: 1) wet, 2) moist, 3) mesic-moist, 4) mesic, and 5) dry according to National Swedish Forest Inventory Instructions (Anon, 2013). To facilitate soil moisture classification in the field, humus layer thickness was measured at sample points using a soil probe and a field ruler. Full definition and characteristics of moisture classes are provided in Table A1. Field data was collected in geopositioned sample points using ESRI application Survey123 (version 3.9) in an iPad Air 2 (8th generation). iPad Airs are equipped with Global Navigation Satellite-based System (GNSS) receivers which uses satellites from the American Global Positioning System (GPS) and the Russian Global Navigation Satellite System (GLONASS). Sample data were collected in the World Geodetic System (WGS-1984) in the field and were later projected with SWEREF99 Transverse Mercator when used in ArcMap. The positioning accuracy achieved by iPad Airs in forest with different tree densities is around 2.5–5 m and improves to 2.5–3 m in clear-cut sites (Hannrup et al., 2020). The first sampling points were randomly selected along the first 50 m of trail on the cut area. A uniform distance of 50 m was then assigned between sampling points, to prevent autocorrelation among observations. A total of 385 sample points were collected in the field.

2.3. LiDAR data and DEM description

Digital elevation models with resolutions of 2 m, 1 m and 0.5 m were created from airbirne LiDAR data with a point density of 0.5–1, 1–2 and 24-point m^{-2}, Fig. 2. Elevation models with resolutions of 2 m and 0.5 m were provided as ready to use raster (TIFF) layers, by the Swedish Mapping, Cadastral and Land Registration Authority and the SCA forest company, respectively. The 1-m resolution DEM was extracted from LiDAR data with 1–2 point m^{-2} (by authors) using Quick Terrain Modeler (INTL, x64), v8.0.4.1 software. Technical specifications of the LiDAR data and DEM extraction algorithms are described in Table 2. In this study, the analysis did not include the measurement errors inherent in each of the LiDAR acquisition techniques, filtering methods and DEM production algorithms, nor how they may affect the accuracy of generated DEMs.

2.4. DTW map production

DTW maps with resolutions corresponding to the DEMs used were created in ArcMap 10.8. Each DEM was first processed to create elevation models with no depressions using a fill function (Tarboton, 1997). The preferential water path from each cell was calculated using a flow direction tool. Flow channels were extracted from DEMs with a deterministic 8 (D8) flow accumulation tool (O'Callaghan and Mark, 1984), using a FIA value of 1 ha. Selecting a 1-ha FIA value allowed us to keep the GIS processing of high-resolution DEMs practical and to produce DTW maps comparable to maps that have been available to the Swedish forestry sector since 2015. It also improved delineation of small temporal flow channels which are mainly activated during high runoff periods, i.e., when snow starts to melt in early spring and/or when rain is the dominant form of precipitation in early autumn (Murphy et al., 2011; Ågren et al., 2015).

The least elevation differences between each surface cell and nearest flow channel, i.e., DTW indexes, were calculated using digital elevation models, slope, and flow channel data layers according to Eq. (1), (Murphy et al., 2007; Murphy et al., 2008):

$$DTW(m) = [\sum((dzi/dxi)a)]Xc \quad (1)$$

$DTW(m)$: Estimated depth to ground water table
dzi/dxi: The least cumulative elevation difference from each cell to the nearest surface water (e.g., the flow channel, or other known watercourses).
a: 1 when movement direction is parallel to the cell edge and 1.414214 when cells are passed diagonally
Xc: resolution of the elevation model, m

2.5. Topographic and DTW index variations of logging sites

The studied logging sites were located on relatively hilly areas, and varied in topographic conditions, i.e., elevation and slope. Mean elevation and slope values, extracted from 2-m DEM, varied between 340.70–419.54 m and 6.68–12.25°respectively among the logging sites, Table 3.

Depth-to-water values <1 m are conventionally considered as potential 'moist' and 'wet' areas for DTW soil moisture mapping in the Swedish landscape (Ågren et al, 2014). These areas were classed in ranges of 0–0.25, 0.26–0.50, 0.51–0.75 and 0.76–1 m and marked in shaded colours in all three variants of the DTW maps over the studied

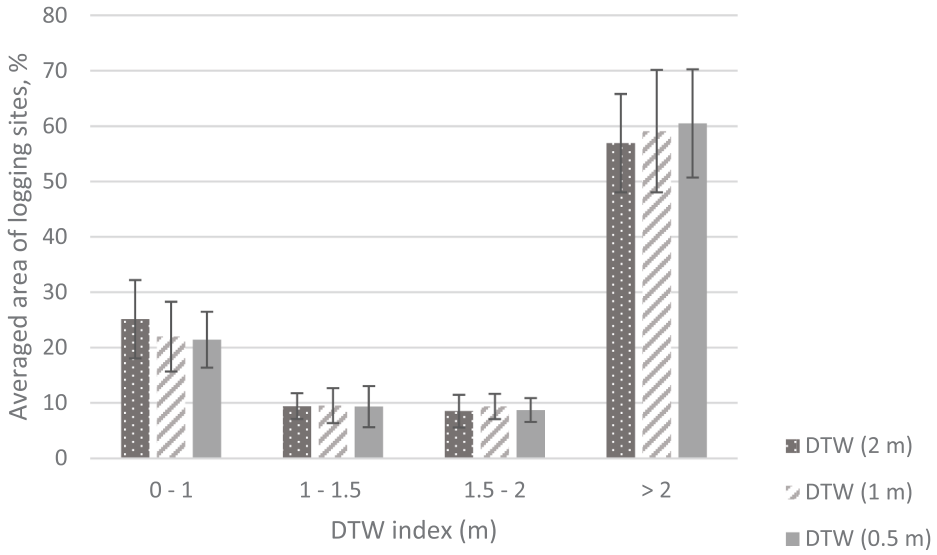

Fig. 3. Distribution of averaged area of logging sites over classes of DTW index. Error bars indicate standard deviation of each DTW index class.

Table 4
Reclassification of DTW maps and field estimated soil moisture classes to binary values, applying conventional DTW threshold value of 1 m to separate wet/dry soils on maps and corresponding soil moisture classes in the field.

DTW reclassification		Field soil moisture reclassification	
Old values	New values	Old values	New values
DTW $\leq$ 1 m	Wet	Wet, moist	Wet
DTW $>$ 1 m	Dry	Mesic-moist, mesic, dry	Dry

logging sites (Table 2A). The averaged area of all logging sites, distributed over the DTW values (0–1, 1–1.5 m, 1.5–2, and $>$ 2 m) on the three resolution maps, are illustrated in Fig. 3. Soils with a DTW index $>$ 2 m made up the major fraction (57–60%) of the areas of all logging sites regardless of DTW map resolutions. Soil moisture condition is considered as 'dry' at these areas, when maps are consulted.

2.6. Data analysis

The average values of the depth-to-water indexes, with a 95% confidence interval, over all the field estimated soil moisture classes were plotted, to evaluate any difference among DTW maps in separating field estimated moisture classes.

In a general linear model, field estimated moisture classes were analysed against DTW index values (from the three map variants, i.e., 2 m, 1 m, and 0.5 m) for all the sample points, to evaluate possible correlations in the soil estimation methods, i.e., field- vs. DTW index estimations. The statistical inferences were performed in Dell Statistica 13.0.

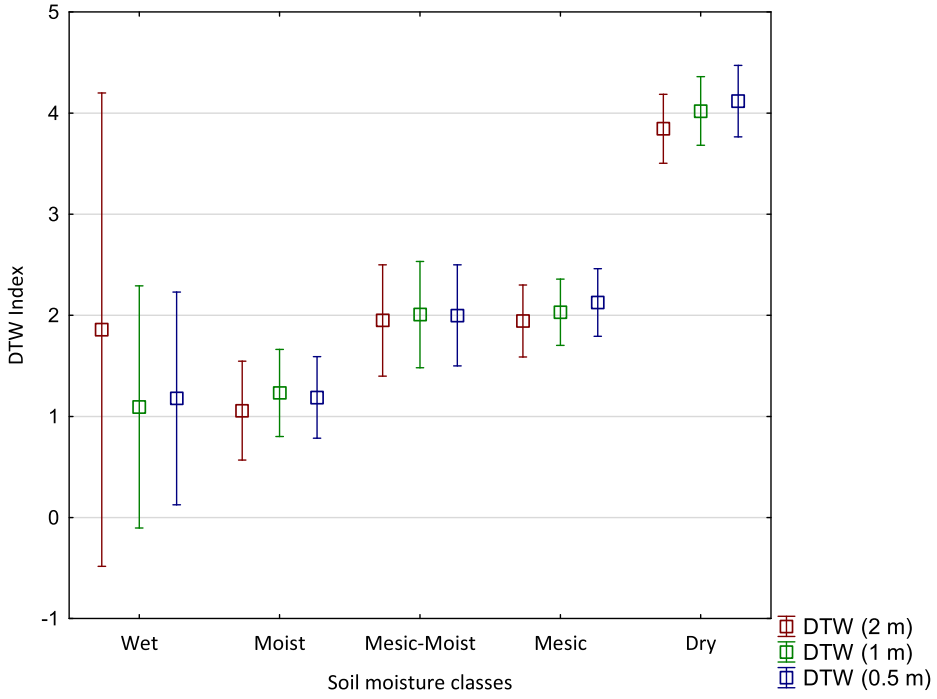

Fig. 4. 95% interval of averaged DTW index values over field estimated soil moisture classes (Anon, 2013), in DTW maps of resolution 2 m, 1 m and 0.5 m.

Table 5
The results of general regression models, where DTW index values were regressed against field estimated soil moisture classes, reporting adjusted R^2, sum of square (SS), degree of freedom (df), F-value and P-value for the models. All three DTW map variants were almost equally effective for distinguishing soil moisture classes in the field.

Dependant variable	Adjusted R^2	SS model	df model	MS model	F	p
DTW (2 m)	0.20	492.92	4	123.23	24.66	< 0.001
DTW (1 m)	0.20	466.56	4	116.64	24.84	< 0.001
DTW (0.5 m)	0.18	426.19	4	106.55	21.65	< 0.001

Table 6
Distribution of True Positive (TP), True Negative (TN), False Positive (FP), False Negative (FN) of DTW maps and corresponding accuracy (ACC, %) and Matthews correlation coefficient (MCC) in DTW maps of resolution 2 m, 1 m and 0.5 m. A DTW threshold value (DTW $\leq$ 1 m) separates wet/dry soil in the maps. Field estimated soil moisture classes wet, and moist are considered as 'Wet'. Number of sample points (n) = 385.

	TP	TN	FP	FN	ACC, %	MCC
DTW (2 m)	25	281	67	12	79	0.33
DTW (1 m)	19	292	56	18	81	0.26
DTW (0.5 m)	21	293	55	16	82	0.30

Table 7
Distribution of True Positive (TP), True Negative (TN), False Positive (FP), False Negative (FN) of DTW maps and corresponding accuracy (ACC, %) and Matthews correlation coefficient (MCC) in DTW maps of resolution 2 m, 1 m and 0.5 m. A new DTW threshold value (DTW $\leq$ 1.5 m) separates wet/dry soil in the maps. Field estimated soil moisture classes wet, moist, mesic-moist, and mesic are considered as 'Wet'. Number of sample points (n) = 385.

	TP	TN	FP	FN	ACC, %	MCC
DTW (2 m)	92	178	71	74	70	0.38
DTW (1 m)	88	188	31	78	72	0.41
DTW (0.5 m)	87	186	33	79	71	0.39

2.7. DTW maps: Performance evaluation

In a more general comparison, DTW values and field estimated moisture values were reclassified to binary values: Wet and Dry. A DTW threshold value of 1 m was used for map reclassification, i.e., all areas with DTW $\leq$ 1 m were reclassed to 'Wet' while areas with DTW > 1 m were reclassed to 'Dry'. The field estimated moisture classes 'wet' and 'moist' were merged to 'Wet' while 'mesic', 'mesic-moist' and 'dry' were merged to the 'Dry' class, Table 4. The averaged area of all logging sites classified as 'Wet' according to this limit in the DTW map reclassification is presented in Fig. 3.

To evaluate the overall conformance of wet areas captured by DTW maps and field-identified wet areas in the new binary classification, accuracy (ACC), and Matthews correlation coefficient (MCC) (Matthews, 1975) were calculated according to Eqs. (2) and (3):

$$ACC = \frac{TP + TN}{TP + TN + FP + FN} \quad (2)$$

$$MCC = \frac{TP \times TN - FP \times FN}{\sqrt{(TP + FP)(TP + FN)(TN + FP)(TN + FN)}} \quad (3)$$

where TP, TN, FP, FN are components of a confusion matrix and are defined as:

True Positive (TP): when both DTW maps and field estimated soil moisture classify the sample as 'Wet'.
True Negative (TN): when both DTW maps and field estimated soil moisture classify the sample as 'Dry'.
False Positive (FP) or type I error: when DTW map reclasses the sample as 'Wet', while soil moisture in field is estimated 'Dry', and
False Negative (FN) or type II error: when DTW map reclasses the sample as 'Dry', while soil moisture in field is estimated 'Wet'.

Finally, the reclassification of soil moisture estimations was iterated with new limits in both DTW maps and field estimations to evaluate possible effects on calculated ACC and MCC in the new classification system. A threshold DTW value of 1.5 m, previously 1 m, was now used to separate 'Wet' and 'Dry' areas in DTW maps, while field estimated soil moisture classes, including 'wet', 'moist', 'mesic-moist', and 'mesic', were reclassified to 'Wet' areas this time.

3. Results

3.1. DTW index value ranges in field estimated soil moisture classes

A comparison between the distribution of DTW indexes and soil moisture classes on each of the DTW maps indicated that all three variants had equivalent performance on separating soil moisture classes estimated in the field. The averaged DTW values were approx. 1.2 m in field moisture class 'wet' and 'moist', approx. 2 m in field moisture class 'mesic-moist' and 'mesic', and approx. 4 m in field moisture class 'dry', Fig. 4. The larger confidence interval for the 2-m resolution DTW index in soil moisture class 'wet' is an effect of one outlier observation being classified as 'wet' in the field while having a DTW value of 4.9 m on the 2-m resolution DTW map.

The averaged DTW index values in the classes 'wet' and 'moist' overlap the values in the classes 'mesic-moist' and 'moist', indicating that DTW maps do not distinguish these soil moisture classes in the field effectively. However, the DTW index in the moisture class 'dry' is efficiently distinguished from other classes.

3.2. Soil moisture prediction by DTW maps

In the general regression models, DTW indexes from all three map variants were regressed against field estimated soil moisture classes. The model resulted in F-values ranging from 21.65 to 24.84 and 24.66 and adjusted R^2-values ranging from 0.18 to 0.20 in the DTW maps with 0.5 m, 1 m, and 2 m resolutions, indicating no improvement in performance of the maps when resolution was improved from 2 m to 1 m and 0.5 m, Table 5.

3.3. Wet and dry soil classification by DTW maps

The accuracy of the binary reclassified ACC of DTW maps in reclassifying the logging sites to 'Wet' and 'Dry' areas increased slightly, from 79% to 81% and 82% in DTW maps with resolutions of 2 m, 1 m, and 0.5 m. The MCC values, however, changed non-uniformly from 0.33 to 0.26 and 0.30 over the studied resolutions respectively (Table 6).

Using the 1.5-m DTW threshold value between wet and dry soil when binary reclassifying DTW maps and field estimated moisture classes, 'wet, moist, mesic-moist and mesic' as the new 'Wet' class, resulted in slightly lower accuracy for all three DTW maps compared to maps with DTW $\leq$ 1 m as the limit between wet and dry areas. The accuracy varied from 70% to 72% and 71% when the resolution of DTW maps was changed from 2 m to 1 m and 0.5 m. Compared to DTW maps with a 1-m limit, the MCC values for these new reclassified DTW maps improved to 0.38, 0.41, and 0.39 (Table 7).

4. Discussion

In this study, we have evaluated how the spatial resolution of the digital elevation models based on different point densities of LiDAR data can affect soil moisture predictions using the DTW soil moisture index.

The pattern and extent of wet and moist areas in maps changed marginally at the studied resolutions and logging sites. The 95% interval of DTW indexes from the spatial resolutions over the field estimated wetness classes showed equivalent distribution of DTW indexes in all three DTW maps. This implies that increased resolution of DEMs at the studied scale, 2 m, 1 m, and 0.5 m, did not affect the performance of the DTW maps in capturing the stream networks and associated wet areas. The higher point density of LiDAR data means more accurate DEMs, with detailed information about surface topography, thereby minimising the need for surface interpolation between the scanning points. This detailed image of the landscape includes small-scale surface features like boulders or stumps, which do not affect the overall pattern of where water would flow in the landscape. DTW maps are created by accounting for differences in gravitational potential energy derived from elevation difference between flow streams and adjacent parts of the landscape. The difference is less affected by changes in microtopography when DEM resolution is increased from 2 m down to 0.5 m, in elevated and hilly areas like the studied logging sites. Large-scale topography is the main controlling factor of water movements in these areas, while detailed surface topography has the main effect in near-surface areas in flat terrains, where DTW maps perform best (Murphy et al., 2009; Schönauer et al., 2021b).

The differences in our DTW maps are not of the same magnitude as that found when 10-m photogrammetry-based DEM were compared to 1-metre LiDAR-based DEMs (Murphy et al., 2008; Murphy et al., 2009). They were not improved in the same way as when (Lidberg et al., 2017) compared resolutions of 2 m, 4 m, 8 m, and 16 m when mapping flow stream networks from hydrologically-corrected LiDAR-based DEMs. Sørensen and Seibert (2007) also reported that higher resolution and information content in 5-m LiDAR-based DEM affected the pattern and distribution of soil moisture estimations by TWI index, compared to 10 m, 25 m, and 50 m LiDAR DEMs. At high resolution DEMs, upslope areas became smaller, contributing to formation of more irregular water flow paths. However, the authors recommended choosing optimum resolution based on the importance of studying topographic features and the soil moisture modelling application.

At higher resolution DEMs, anthropogenic features of landscapes like road banks, railways and ditches may have greater impact on the accuracy of DEMs, so the need to pre-process these models and hydrological modification is more pronounced (Lindsay & Dhun, 2015). Breaching was found to be an optimum algorithm for performing hydrological corrections in DEMs prior to soil moisture modelling (Lidberg et al., 2017). However, we applied “filling” in our DTW map productions, to keep their conformance to DTW-maps available for the whole of Sweden. Slight variations in captured patterns of flow channels and associated wet areas at studied resolutions might therefore be explained by different sensitivity of these DEMs to artefacts like road banks close to the logging sites (Table A2, logging sites 1, 2, 4, 6 and 7). However, the differences were quite minimal and did not result in considerable variation in the soil moisture maps created here at the studied scales.

The comparison of DTW indexes and field estimated soil moisture classes also indicated that DTW maps were more effective in distinguishing dry areas, with DTW $\geq$ 4 m from the other moisture classes (Fig. 4). DTW values in the wet and moist soil moisture classes (0.02 m $<$ DTW $<$ 2 m) and mesic-moist and mesic (1.5 m $<$ DTW $<$ 2.5 m) overlap to a great extent, making the index ineffective in separating these soil moisture classes. This was also confirmed by results from the general linear model, where DTW index values regressed by field estimated soil moisture classes produced low adjusted R^2 values for all resolutions. However, this might partly be an effect of the resolution of the field classification of soil moisture, where many of the recognition signs are related to an area surrounding the sample point and not just the sample point itself. Furthermore, as soil moisture is a continuous variable, the transitions between classes will be gradual and not well defined at specific boundaries.

The accuracy (ACC) of DTW maps slightly improved, from 79% to 80% and 81% respectively, regarding reclassifying the soil moisture to the binary values of ‘Wet’ and ‘Dry’ in maps and the field, when resolution was increased from 2 m to 1 m and 0.5 m. This was mainly due to the increased number of observations in the True Negative and True Positive classes, i.e., correctly classified field sample points in moisture classes ‘Dry’ and ‘Wet’ by the DTW maps. However, the MCC value did not improve. When the resolution was changed from 2 m to 1 m and 0.5 m, MCC was reduced from 0.33 to 0.26 and increased to 0.30, contrasting with the marginal improvement of accuracy (ACC). The records are not far from values reported in two areas with similar soil deposits, i.e., till and peat studied by Ågren et al. (2014), with ACC = 83.9% and 77.5% and MCC = 0.39 and 0.34.

Modifying the applied threshold for reclassification of DTW index and field estimated soil moisture classes, i.e., DTW $\leq$ 0 1.5 and field classes as wet, moist, moist-mesic, and mesic, resulted in reduced ACC but improved MCC for all resolutions of DTW maps, compared with the previous classification trial. The best MCC improvement was found for DTW (1 m), from 0.26 to 0.41. This would indicate that applying a DTW threshold value $\leq$ 1 m is not always the best practice to identify sensitive areas around flow channels, and the limit needs to be adjusted to local topographic conditions (Ågren et al., 2021).

Mesic-moist and mesic soil moisture classes indicate more temporal variations during a year, having least bearing capacity (more wet and moist areas) during early spring and late autumn. Soils of these moisture classes may have higher bearing capacity when the soil is drier during summer. Therefore, including actual meteorological data, like field measured or hydrologically modelled soil temperature and moisture content, could be a possible approach to generate more dynamic DTW maps (Jones & Arp, 2019). Real time data about actual soil strength by automatic indirect measuring methods, such as harvesters’ CAN-BUS measurements of rolling resistance (Ala-Ilomäki et al., 2020) prior to forwarding operations, can also be used as a complement to static soil moisture models. Real time measurement of soil strength, together with spatial data and hydrological modelling, can also provide dynamic soil trafficability maps (Salmivaara et al., 2020). These types of maps are increasingly demanded by forestry to minimise the negative impacts of machinery operations on soils in more fluctuating weather conditions.

Identifying optimal FIA values for different scales of application has been recognised as challenging, due to spatial and temporal variations in soil moisture content (Lidberg et al., 2020). In a study by Schönauer et al. (2021b), field-measured soil moisture content and soil strength in time series under different weather conditions in boreal and temperate forest sites in Germany, Poland, and Finland were compared to DTW maps with varying FIA values. DTW performance in predicting soil moisture condition was best at FIA = 4 ha. The map performance, however, did not improve overall with site- and condition-adjusted FIA values.

The somewhat low conformance of the maps to field estimated moisture classes found in this study may also be because we applied a constant flow initiation threshold of 1 ha for extraction of the flow

channels over all studied logging sites, without making any modifications based on local topographic and temporal condition. This FIA may result in DTW maps overestimating wet areas in steep terrain conditions or in soils with high drainage properties (Lidberg et al., 2020; Murphy et al., 2009). This effect is more pronounced in DTW maps with 2-m resolution, with higher False Positive values (FP = 67) compared to FP = 56 and FP = 55 at 1 m and 0.5 m resolutions (with DTW $\leq$ 1 m as threshold value for wet/dry soils). When mapping small stream networks (<6 m wide) at a national scale in Sweden, a FIA value of 2 ha is recommended (Ågren & Lidberg, 2019). However, much smaller, seasonally activated, water flow paths at logging site scales may not be captured at this FIA value.

New techniques, such as machine learning, enable inclusion of more site- and time-specific information like hydrological measurements or multiple topographic wetness index. This improves the development of regionally adjusted wet area maps at local and national scales (Lidberg et al., 2020; Ågren et al., 2021).

A higher spatial resolution of the DEMs did not effectively change the accuracy of DTW maps in identifying wet and moist areas in forest soil in elevated and hilly topography. However, DTW maps based on extracted flow channels from LiDAR-based DEMs have greatly improved mapping of flow-channels and associated wet areas compared to conventional methods using aerial photography. Capturing integrated flow channels based on detailed DEMs can improve planning of logging operations, by identifying possible wet areas near surface waters and applying modified log extraction methods in these areas. Developing dynamic DTW maps through inclusion of hydrological and weather data may also improve scheduling of logging operations in these areas to periods with improved soil strength.

5. Conclusion

The results of our study confirm that higher resolution of digital elevation models (considering 2-m, 1-m, and 0.5-m resolutions) based on high-density airborne LiDAR data does not imply improvement in identifying wet and moist areas in forest soils in relatively elevated and hilly terrain using the DTW soil moisture index. The overall pattern of subsurface water movement is mainly influenced by large-scale topography over these types of terrains, and not by detailed surface topography, as on flat areas. DEM resolution of 1–2 m can therefore be considered as sufficient for application in planning of logging or other forestry operations in terrains with similar properties, where knowledge about soil hydrological features, and associated wet and moist areas and their connectivity, is beneficial.

CRediT authorship contribution statement

Sima Mohtashami: Conceptualization, Data curation, Formal analysis, Investigation, Resources, Methodology, Project administration, Software, Validation, Visualization, Writing – original draft, Writing – review & editing. **Lars Eliasson:** Conceptualization, Funding acquisition, Methodology, Supervision, Writing – review & editing. **Linnea Hansson:** Conceptualization, Methodology, Supervision, Writing – review & editing. **Erik Willén:** Conceptualization, Writing – review & editing, Project administration. **Tomas Thierfelder:** Conceptualization, Formal analysis, Methodology, Supervision, Software, Writing – review & editing. **Tomas Nordfjell:** Conceptualization, Formal analysis, Methodology, Writing – review & editing.

Declaration of Competing Interest

The authors declare that they have no known competing financial interests or personal relationships that could have appeared to influence the work reported in this paper.

Acknowledgement

The authors thank the Research Foundation Nils & Dorthi Troedssons for financing the project, SCA for hosting and providing us with logging sites and high-resolution LiDAR data, and Greensway for helping us with data collection on logging sites during Oct-Nov 2020.

Appendix A

See Tables A1 and A2.

Table A1
Definition of soil moisture classes with recognition signs in forest, according to National Swedish Forest Inventory Instructions (Anon, 2013).

Soil moisture classes	Groundwater Level (GWL)	Recognition signs in forest
Wet soils	GWL at soil surface	(1) Organic soils (often fens). (2) Conifers occur only occasionally. (3) Frequent permanent water pools. (4) One cannot walk dry footed in low shoes.
Moist soils	GWL < 1 m depth	(1) Soils range from organic (generally fens) to mineral (generally humus-podsol). (2) Wetland mosses dominate local depressions (pits), and trees often show a coarse root system above ground. (3) One can walk dry footed in low shoes, provided one can step on tussocks in the wetter parts. (4) Ditches are common.
Mesic-moist soils	GWL < 1 m depth	(1) Soils are podzolic (humo-ferric to humic podsols) (2) The mineral soil is covered by a thick peaty mor (thicker than mesic soils) (3) Wetland mosses are common (4) Trees show a coarse root system above ground (germination point above soil) (5) One can walk dry footed in low shoes over the entire vegetation area, expect after heavy rain or snowmelt.
Mesic soils	1 m < GWL < 2 *m*	(1) Ferric podsols with a thin humus layer (mor) are common. (2) The bleached horizon is grey-white and well delineated against the rust yellow, rust-red or brownish rust-red B-horizon (the darker the colour, the wetter the soil). (3) The bottom layer consists mainly of dryland mosses. (4) One can walk dry-footed in low shoes over the area even after heavy rains/snowmelt.
Dry soils	GWL > 2 *m*	(1) Usually found on eskers, hills, marked crowns and ridge crests (2) Soils tend to be coarse in texture and include lithosol, boulder soil and iron podsol formations, generally covered with a thin humus blanket on a thin bleached horizon. (3) Significant bedrock exposure.

Table A2

Comparison of DTW maps over eight logging sites, presented on topographic map of Sweden. DTW maps with resolutions of 2 m, 1 m, and 0.5 m, are extracted from DEMs with corresponding resolution. Wet areas with DTW index values 0–0.25, 0.26–0.50, 0.51–0.75 and 0.76–1 m are shaded on the DTW maps. Flow initiation area (FIA) was defined as 1 ha for all DTW maps.

Logging site 1	Logging site 2	Logging site 3	Logging site 4	
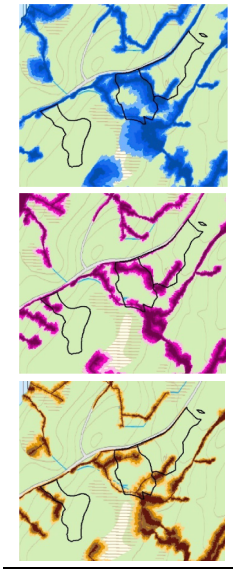	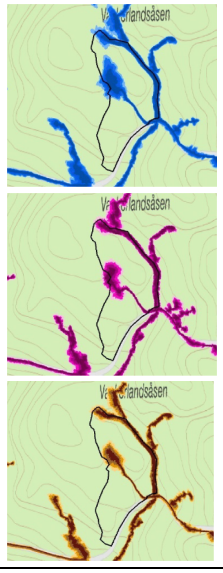	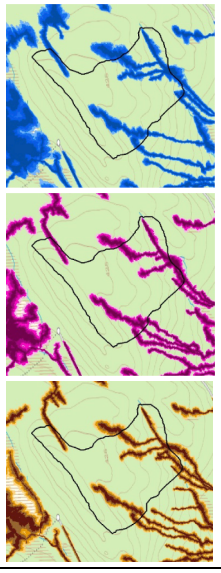	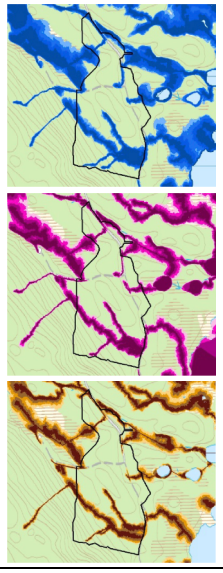	DTW (2 m) 0 - 0.25 0.26 - 0.50 0.51 - 0.75 0.76-1 DTW (1 m) 0 - 0.25 0.26 - 0.50 0.51 - 0.75 0.76 - 1 DTW (0.5 m) 0 - 0.25 0.26 - 0.50 0.51 - 0.75 0.76 - 1
Logging site 5	**Logging site 6**	**Logging site 7**	**Logging site 8**	
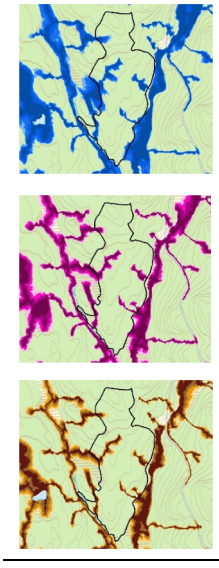	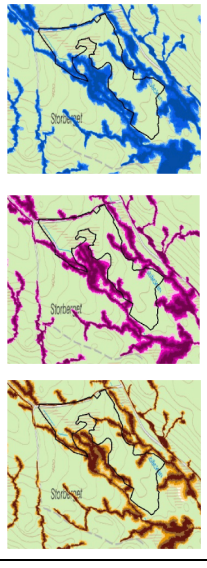		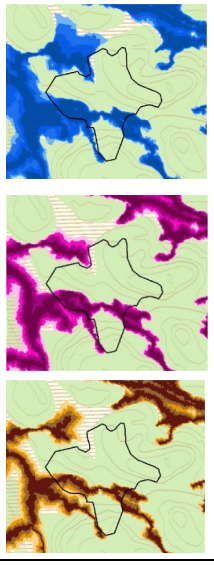	DTW (2 m) 0 - 0.25 0.26 - 0.50 0.51 - 0.75 0.76-1 DTW (1 m) 0 - 0.25 0.26 - 0.50 0.51 - 0.75 0.76 - 1 DTW (0.5 m) 0 - 0.25 0.26 - 0.50 0.51 - 0.75 0.76 - 1

References

Ala-Ilomäki, J., Salmivaara, A., Launiainen, S., Lindeman, H., Kulju, S., Finér, L., Heikkonen, J., Uusitalo, J., 2020. Assessing extraction trail trafficability using harvester CAN-bus data. Int. J. For. Eng. 31 (2), 138–145. https://doi.org/10.1080/14942119.2020.1748958.

Ågren, A., Lidberg, W., Ring, E., 2015. Mapping Temporal Dynamics in a Forest Stream Network—Implications for Riparian Forest Management. Forests 6 (9), 2982–3001. https://doi.org/10.3390/f6092982.

Ågren, A.M., Larson, J., Paul, S.S., Laudon, H., Lidberg, W., 2021. Use of multiple LIDAR-derived digital terrain indices and machine learning for high-resolution national-scale soil moisture mapping of the Swedish forest landscape. Geoderma 404, 115280. https://doi.org/10.1016/j.geoderma.2021.115280.

Ågren, A.M., Lidberg, W., 2019. The importance of better mapping of stream networks using high resolution digital elevation models_ Upscaling from watershed scale to regional and national scales. Hydrol. Earth Syst. Sci. Discuss. 1–20 https://doi.org/10.5194/hess-2019-34.

Ågren, A.M., Lidberg, W., Strömgren, M., Ogilvie, J., Arp, P.A., 2014. Evaluating digital terrain indices for soil wetness mapping – a Swedish case study. Hydrol. Earth Syst. Sci. 18 (9), 3623–3634. https://doi.org/10.5194/hess-18-3623-2014.

Anon., 2013. Riksinventering av skog, Fältinstruktion 2013. Department of Forest Resource Management and Department of Soil and Environment, Umeå, Uppsala.

Anon., 2020. Produktbeskrivning GSD höjddata, Grid 2+. Lantmäteriet. Retrieved 25 January 2022 from: https://www.lantmateriet.se/globalassets/kartor-och-geografisk-information/hojddata/hojd2_plus_2.8.pdf.

Anon., 2021. Produktbeskrivning, LaserData Nedladdning Skog. Lantmäteriet. Retrieved 25 January 2022 from: https://www.lantmateriet.se/globalassets/kartor-och-geografisk-information/hojddata/pb_laserdata_nedladdning_skog.pdf.

Anon., 2022. RIEGL laser measurement system. Retrieved 14 January 2022 from: http://www.riegl.com/nc/products/airborne-scanning/produktdetail/product/scanner/55/.

Arp, P.A., 2009. High resolution flow-channel and wet-areas maps: a tool for better forest operations planning, Sustainable Forest Management Network, SFM Network Research Note.

Beven, K.J., Kirkby, M.J., 1979. A physically based, variable contributing area model of basin hydrology/Un modèle à base physique de zone d'appel variable de l'hydrologie du bassin versant. Hydrol. Sci. Bull. 24 (1), 43–69. https://doi.org/10.1080/02626667909491834.

Cambi, M., Certini, G., Neri, F., Marchi, E., 2015. The impact of heavy traffic on forest soils: A review. For. Ecol. Manage. 338, 124–138. https://doi.org/10.1016/j.foreco.2014.11.022.

Campbell, D.M.H., White, B., Arp, P.A., 2013. Modeling and mapping soil resistance to penetration and rutting using LiDAR-derived digital elevation data. J. Soil Water Conserv. 68 (6), 460–473. https://doi.org/10.2489/jswc.68.6.460.

DeArmond, D., Ferraz, J.B.S., Higuchi, N., 2021. Natural recovery of skid trails: a review. Can. J. For. Res. 51 (7), 948–961. https://doi.org/10.1139/cjfr-2020-0419.
Eliasson, L., Wästerlund, I., 2007. Effects of slash reinforcement of strip roads on rutting and soil compaction on a moist fine-grained soil. For. Ecol. Manage. 252 (1–3), 118–123. https://doi.org/10.1016/j.foreco.2007.06.037.
Friberg, G., Bergkvist, I., 2016. Så påverkar arbetsrutiner och markfuktighetskartor körskador i skogsbruket [How operational procedures and depth-to-water maps can reduce damage on soil and water and rutting in the Swedish forestry]. Skogforsk, Uppsala.
Grabs, T., Seibert, J., Bishop, K., Laudon, H., 2009. Modeling spatial patterns of saturated areas: A comparison of the topographic wetness index and a dynamic distributed model. J. Hydrol. 373 (1-2), 15–23. https://doi.org/10.1016/j.jhydrol.2009.03.031.
Hannrup, B., Ene, L., Johansson, F., Jönsson, P., Rossander, M., Willén, E., 2020. Utvärdering av nya möjligheter till förbättrad positionering med satellitbaserade system [Evaluation of potential for improved positioning with satellite-based systems]. Skogforsk, Uppsala.
Hansson, L.J., Koestel, J., Ring, E., Gärdenäs, A.I., 2018. Impacts of off-road traffic on soil physical properties of forest clear-cuts: X-ray and laboratory analysis. Scand. J. For. Res. 33 (2), 166–177. https://doi.org/10.1080/02827581.2017.1339121.
Hjerdt, K.N., McDonnell, J.J., Seibert, J., Rodhe, A., 2004. A new topographic index to quantify downslope controls on local drainage. Water Resour. Res. 40, W05602(5). https://doi.org/10.1029/2004wr003130.
Hoffmann, S., Schönauer, M., Heppelmann, J., Asikainen, A., Cacot, E., Eberhard, B., Hasenauer, H., Ivanovs, J., Jaeger, D., Lazdins, A., Mohtashami, S., Moskalik, T., Nordfjell, T., Stereńczak, K., Talbot, B., Uusitalo, J., Vuillermoz, M., Astrup, R., 2022. Trafficability prediction using Depth-to-Water Maps: the Status of application in northern and central European forestry. Curr. For. Rep. https://doi.org/10.1007/s40725-021-00153-8.
Huisman, J.A., Snepvangers, J.J.J.C., Bouten, W., Heuvelink, G.B.M., 2002. Mapping spatial variation in surface soil water content: comparison of ground penetrating radar and time domain reflectromatry. J. Hydrol. 269, 194–207.
Jones, M.-F., Arp, P., 2019. Soil Trafficability Forecasting. Open J. For. 09 (04), 296–322. https://doi.org/10.4236/ojf.2019.94017.
Kuglerová, L., Hasselquist, E.M., Richardson, J.S., Sponseller, R.A., Kreutzweiser, D.P., Laudon, H., 2017. Management perspectives on Aqua incognita: Connectivity and cumulative effects of small natural and artificial streams in boreal forests. Hydrol. Process. 31 (23), 4238–4244. https://doi.org/10.1002/hyp.11281.
Kuglerová, L., Ågren, A., Jansson, R., Laudon, H., 2014. Towards optimizing riparian buffer zones: Ecological and biogeochemical implications for forest management. For. Ecol. Manage. 334, 74–84. https://doi.org/10.1016/j.foreco.2014.08.033.
Labelle, E.R., Hansson, L., Högbom, L., Jourgholami, M., Laschi, A., 2021. Strategies to mitigate the effects of soil physical disturbances caused by forest machinery: a comprehensive review. Current Forestry Report. In press.
Lehtonen, I., Venäläinen, A., Kämäräinen, M., Asikainen, A., Laitila, J., Anttila, P., Peltola, H., 2019. Projected decrease in wintertime bearing capacity on different forest and soil types in Finland under a warming climate. Hydrol. Earth Syst. Sci. 23 (3), 1611–1631. https://doi.org/10.5194/hess-23-1611-2019.
Lekshmi, S.U., Susha, Singh, D.N., Shojaei Baghini, M., 2014. A critical review of soil moisture measurement. Measurement 54, 92–105. https://doi.org/10.1016/j.measurement.2014.04.007.
Lidberg, W., Nilsson, M., Ågren, A., 2020. Using machine learning to generate high-resolution wet area maps for planning forest management: A study in a boreal forest landscape. Ambio 49 (2), 475–486. https://doi.org/10.1007/s13280-019-01196-9.
Lidberg, W., Nilsson, M., Lundmark, T., Ågren, A.M., 2017. Evaluating preprocessing methods of digital elevation models for hydrological modelling. Hydrol. Process. 31 (26), 4660–4668. https://doi.org/10.1002/hyp.11385.
Lindsay, J.B., Dhun, K., 2015. Modelling surface drainage patterns in altered landscapes using LiDAR. Int. J. Geograph. Inform. Sci. 29 (3), 397–411. https://doi.org/10.1080/13658816.2014.975715.
Lunt, I.A., Hubbard, S.S., Rubin, Y., 2005. Soil moisture content estimation using ground-penetrating radar reflection data. J. Hydrol. 307 (1–4), 254–269. https://doi.org/10.1016/j.jhydrol.2004.10.014.
MacMillan, R.A., Martin, T.C., Earle, T.J., McNabb, D.H., 2014. Automated analysis and classification of landforms using high-resolution digital elevation data: applications and issues. Can. J. Remote Sens. 29 (5), 592–606. https://doi.org/10.5589/m03-031.
Matthews, B.W., 1975. Comparison of the predicted and observed secondary structure of T4phage lysozyme. BBA 405 (2), 442–451.
Mattila, U., Tokola, T., 2019. Terrain mobility estimation using TWI and airborne gamma-ray data. J. Environ. Manage. 232, 531–536. https://doi.org/10.1016/j.jenvman.2018.11.081.
Mohtashami, S., Eliasson, L., Jansson, G., Sonesson, J., 2017. Influence of soil type, cartographic depth-to-water, road reinforcement and traffic intensity on rut formation in logging operations: a survey study in Sweden. Silva Fennica 51 (5). https://doi.org/10.14214/sf.2018.
Murphy, P.N.C., Ogilvie, J., Meng, F.-R., Arp, P., 2008. Stream network modelling using lidar and photogrammetric digital elevation models: a comparison and field verification. Hydrol. Process. 22 (12), 1747–1754. https://doi.org/10.1002/hyp.6770.
Murphy, P.N.C., Ogilvie, J., Arp, P., 2009. Topographic modelling of soil moisture conditions: a comparison and verification of two models. Eur. J. Soil Sci. 60 (1), 94–109. https://doi.org/10.1111/j.1365-2389.2008.01094.x.
Murphy, P.N.C., Ogilvie, J., Connor, K., Arp, P.A., 2007. Mapping wetlands: a comparison of two different approaches for New Brunswick, Canada. Wetlands 27 (4), 846–854.
Murphy, P.N.C., Ogilvie, J., Meng, F.-R., White, B., Bhatti, J.S., Arp, P.A., 2011. Modelling and mapping topographic variations in forest soils at high resolution: A case study. Ecol. Model. 222 (14), 2314–2332. https://doi.org/10.1016/j.ecolmodel.2011.01.003.
Najafi, A., Solgi, A., Sadeghi, S.H., 2009. Soil disturbance following four wheel rubber skidder logging on the steep trail in the north mountainous forest of Iran. Soil Tillage Res. 103 (1), 165–169. https://doi.org/10.1016/j.still.2008.10.003.
Nordfjell, T., Öhman, E., Lindroos, O., Ager, B., 2019. The technical development of forwarders in Sweden between 1962 and 2012 and of sales between 1975 and 2017. Int. J. For. Eng. 30 (1), 1–13. https://doi.org/10.1080/14942119.2019.1591074.
O'Callaghan, J.F., Mark, D.M., 1984. The extraction of drainage networks from digital elevation data. Comp. Vis. Graph. Image Process. 28 (3), 323–344.
Ring, E., Ågren, A., Bergkvist, I., Finér, L., Johansson, F., Högbom, L., 2020. A guide to using wet area maps in forestry. Skogforsk, Uppsala.
Salmivaara, A., Launiainen, S., Perttunen, J., Nevalainen, P., Pohjankukka, J., Ala-Ilomäki, J., Sirén, M., Laurén, A., Tuominen, S., Uusitalo, J., Pahikkala, T., Heikkonen, J., Finér, L., 2020. Towards dynamic forest trafficability prediction using open spatial data, hydrological modelling and sensor technology. For. Int. J. For. Res. 93 (5), 662–674. https://doi.org/10.1093/forestry/cpaa010.
Schönauer, M., Hoffmann, S., Maack, J., Jansen, M., Jaeger, D., 2021a. Comparison of selected terramechanical test procedures and cartographic indices to predict rutting caused by machine traffic during a Cut-to-Length thinning Operation. Forests 12 (2), 113. https://doi.org/10.3390/f12020113.
Schönauer, M., Väätäinen, K., Prinz, R., Lindeman, H., Pszenny, D., Jansen, M., Maack, J., Talbot, B., Astrup, R., Jaeger, D., 2021b. Spatio-temporal prediction of soil moisture and soil strength by depth-to-water maps. Int. J. Appl. Earth Obs. Geoinf. 105, 102614. https://doi.org/10.1016/j.jag.2021.102614.
Sirén, M., Salmivaara, A., Ala-Ilomäki, J., Launiainen, S., Lindeman, H., Uusitalo, J., Sutinen, R., Hänninen, P., 2019. Predicting forwarder rut formation on fine-grained mineral soils. Scand. J. For. Res. 34 (2), 145–154. https://doi.org/10.1080/02827581.2018.1562567.
Susnjar, M., Horvat, D., Seselje, J., 2006. Soil compaction in timber skidding in winter conditions. Croat. J. For. Eng. 27 (1), 3–15.
Sørensen, R., Seibert, J., 2007. Effects of DEM resolution on the calculation of topographical indices: TWI and its components. J. Hydrol. 347 (1–2), 79–89. https://doi.org/10.1016/j.jhydrol.2007.09.001.
Tarboton, D.G., 1997. A new method for the determination of flow directions and upslope areas in grid digital elevation models. Water Resour. Res. 33 (2), 309–319. https://doi.org/10.1029/96wr03137.
Toivio, J., Helmisaari, H.-S., Palviainen, M., Lindeman, H., Ala-Ilomäki, J., Sirén, M., Uusitalo, J., 2017. Impacts of timber forwarding on physical properties of forest soils in southern Finland. For. Ecol. Manage. 405, 22–30. https://doi.org/10.1016/j.foreco.2017.09.022.
Uusitalo, J., Ala-Ilomäki, J., 2013. The significance of above-ground biomass, moisture content and mechanical properties of peat layer on the bearing capacity of ditched pine bogs. Silva Fennica 47 (3). https://doi.org/10.14214/sf.993.
Uusitalo, J., Ala-Ilomäki, J., Lindeman, H., Toivio, J., Siren, M., 2020. Predicting rut depth induced by an 8-wheeled forwarder in fine-grained boreal forest soils. Ann. For. Sci. 77 (2) https://doi.org/10.1007/s13595-020-00948-y.
White, B., Ogilvie, J., Campbell, D.M.H.M.H., Hiltz, D., Gauthier, B., Chisholm, H.K.H., Wen, H.K., Murphy, P.N.C.N.C., Arp, P.A.A., 2013. Using the Cartographic Depth-to-Water Index to Locate Small Streams and Associated Wet Areas across Landscapes. Can. Water Resour. J./Revue canadienne des ressources hydriques 37 (4), 333–347. https://doi.org/10.4296/cwrj2011-909.
Wästerlund, I., 2020. Soil mechanics for forestry ground and measurements. In: Soil and Root Damage in Forestry. Elsevier, pp. 113–137. https://doi.org/10.1016/b978-0-12-822070-2.00006-7.
Wehr, A., Lohr, U., 1999. Airborne laser scanning-an introduction and overview. ISPRS J. Photogrammetr. Remote Sens. 54, 68–82.